

Analysis of CO₂ and O₂ in soil gas over faults and fractures and associated with volcanic massive sulphide and porphyry-style mineralization in British Columbia, Canada

Ray Lett^{1,*}, Dave Sacco² and Cameron Knox²

¹ 3956 Ashford Road, Victoria, British Columbia, Canada, V8P 3S5

² SLR Consulting (Canada) Ltd., 887 Great Northern Way, Suite 200, Vancouver, British Columbia, Canada, V5T 4T5

* Corresponding author's e-mail: Raylett@shaw.ca

<https://doi.org/10.70499/VHGY8023>

ABSTRACT

Soil gases over the Mouse Mountain Cu-Au porphyry occurrence, the Mount Milligan Cu-Au deposit, and the Anita Cu-Pb-Zn-Au-Ag VMS mineral property in British Columbia, Canada, were analyzed for carbon dioxide (CO₂) and oxygen (O₂). During each survey, soil gas was analyzed in real-time after being pumped through a hollow steel tube driven roughly 40 cm into the soil. At Mouse Mountain and Mount Milligan, the CO₂ and O₂ concentrations in soil gas were determined with a custom-built measurement system, whereas the commercially available CO₂Meter GasLab[®] Pro Multi-Gas CM 1000 Data Logger[™] was used to measure CO₂, O₂, and methane (CH₄) on the Anita property. Duplicate analyses across test sites indicate that CO₂ and O₂ values obtained from the two analytical systems are comparable; however, the CM 1000 Data Logger has a higher O₂ detection limit of 100 ppm, compared to the 10 ppm detection limit for the custom-built system.

Three metrics were calculated for data display and interpretation: ΔCO_2 , ΔO_2 , and $\Delta\text{CO}_2\&\text{O}_2$. The ΔCO_2 and ΔO_2 values represent soil gas CO₂ and O₂ concentrations after compensation for atmospheric CO₂ and O₂ levels. Typically, CO₂ in soil gas increases over a fault with an associated decrease in O₂; therefore, $\Delta\text{CO}_2\&\text{O}_2$ is used as a single measure of the total ΔCO_2 and ΔO_2 variability, providing a higher contrast anomaly. There is a strong spatial correlation of positive ΔCO_2 and negative ΔO_2 soil gas anomalies with fractures that were mapped in a bedrock trench at Mount Milligan and with the faults projected from the bedrock geology at Anita.

At Mouse Mountain, fault locations are inferred from the survey results, assuming a spatial relationship between structure and soil gas chemistry. Soil samples were also collected at Mouse Mountain, which underwent a multi-element geochemical analysis with an inductively coupled plasma mass spectrometer following a water leach. Higher water-soluble sulphur levels spatially associated with a $\Delta\text{CO}_2\&\Delta\text{O}_2$ peak could indicate the release of SO₂, carbon disulphide and carbonyl sulphide from oxidizing, fault-hosted sulphide minerals. The positive relationship suggests that a field analysis of a soil-water leach for SO₄ could be completed in combination with soil gas CO₂ and O₂ measurements to differentiate sulphide mineralized faults from non-mineralized faults. The current research indicates portable CO₂ and O₂ sensors can be effectively used to detect buried structures and, with the addition of other gases, may be used to differentiate mineralized structures.

INTRODUCTION

Identifying bedrock faults that underlie glacial sediments can be challenging, even when supported by surface bedrock mapping, geophysics, and remote sensing. Recently, the analysis of soil gas for mercury (Hg) (Rukhlov et al. 2021), methane (CH₄), carbon dioxide (CO₂) and oxygen (O₂) (Lett et al. 2022) has been used to detect buried faults and associated sulphide minerals beneath residual and transported overburden. Previously, Lovell et al. (1979, 1980) reported higher CO₂ and decreasing O₂ in the soil gas sampled in Ireland over Pb-Zn sulphide-mineralized faults buried beneath thick glacial sediments. McCarthy et al. (1986) also found elevated CO₂ and lower O₂ in the soil gas sampled over the Crandon massive sulphide deposit that is buried under 65 m of glacial sediments in Wisconsin, USA. Highsmith (2004) proposed a model to explain the formation of soil gas CO₂ and O₂ anomalies over geological structures and sulphide-bearing faults. Kesler et al. (1990) studied the dispersion of soil gas from gold deposits. Higher concentrations of CO₂ in soil gas can also be caused through leakage from geological CO₂ storage sites (Annunziatellis et al. 2008).

continued on page 5



ORCID Numbers

Ray Lett <https://orcid.org/0009-0008-8782-5887>

Dave Sacco *no ORCID number*

Cameron Knox *no ORCID number*

CO₂ and O₂ in soil gas over faults, fractures and associated with mineralization *continued from p 1*

A secondary effect of the CO₂ migrating to surface may be a change in soil mineral chemistry, such as the formation of secondary carbonate minerals and soil pH anomalies (Smee 1998). Beaubien (2008) reported soil pH as low as 3.5, accompanied by the absence of surface vegetation on a Mediterranean pasture over a natural CO₂ gas vent in the LATERA geothermal field, central Italy. However, Zhao et al. (2017) detected only a modest pH change from 7.91 to 8.17 in the soil sampled over gas vents on the Qinghai-Tibet Plateau, where CO₂ concentrations ranged from 500 to 12 000 ppm. Incidentally, soil SO₄ decreased with increasing soil CO₂. These coincident results may provide additional context for interpreting CO₂ anomalies.

Hale (2010) and, more recently, Plet and Nobel (2023) reviewed soil-gas chemistry and its application to mineral exploration, noting that previous surveys either measured soil gas CO₂ and O₂ concentrations on-site (e.g. Lovell et al. 1980) or collected a soil gas sample for subsequent laboratory analysis (e.g. McCarthy et al. 1986). Real-time soil gas surveys can be valuable to mineral exploration programs because they provide data that can be used to revise and focus programs while work is underway. Unfortunately, past commercial devices for the field-based analysis of CO₂ and O₂ have been cumbersome and expensive. Soil gas can also be sampled, captured and stored in a container on site for later laboratory analysis for CO₂, O₂ and for other elements (e.g. He), but this approach introduces risks of sample contamination during transport and delays the reporting of survey results, which precludes immediate follow-up while still in the field.

A project initiated in 2019 and funded by Geoscience BC led to the development of a portable, real-time soil gas measurement system. The prototype device used small, commercially available sensors from CO2Meter Inc.™ to measure CO₂ and O₂ in atmospheric air and in soil gas. Subsequently, an improved version of the system, informally named 'SGAS', was developed. The development process is described in Lett et al. (2020, 2022). CO2Meter Inc.™ has also developed a compact handheld device, the CO2Meter GasLab® Pro Multi-Gas Sampling CM 1000 Data Logger ('CM 1000 Data Logger'), which measures CO₂, O₂, and CH₄ in soil gas. Herein, we describe the results of analyzing soil gas with both the SGAS and CM 1000 Data Logger systems. The two systems were first tested at an urban site to compare their functionality. Subsequently, the SGAS system was used to complete soil gas surveys over porphyry Cu-Au mineralization at the Mouse Mountain mineral property and at the Mount Milligan Cu-Au mine, and the CM 1000 logger was employed over volcanic massive Cu-Pb-Zn-Au-Ag sulphide mineralization at the Anita volcanic massive sulphide (VMS) mineral property, British Columbia (Fig. 1).

SGAS measurement system

Development and testing of the SGAS system is detailed in Lett et al. (2020, 2022). The sensor unit, housed in a waterproof case, has a SprintIR®-6S 5%CO₂ Smart sensor and a UV Flux 25% Oxygen Smart Flow O₂ sensor mounted on a circuit board (Fig. 2). In addition to CO₂ and O₂ concentrations, sensors also measure barometric pressure, temperature and relative humidity. Each sensor body has an inlet and an exit port to attach flexible PVC tubes. One inlet

Note: This EXPLORE article has been extracted from the original EXPLORE Newsletter. Therefore, page numbers may not be continuous and any advertisement has been masked.



Fig. 1. Mouse Mountain, Mount Milligan, and Anita project locations in British Columbia, Canada.

continued on page 6

CO₂ and O₂ in soil gas over faults, fractures and associated with mineralization *continued from p. 5*

port on the CO₂ sensor manifold is connected by a PVC tube to a corresponding exit port on the O₂ sensor so that the gas can flow continuously into the two linked sensors. Each sensor circuit board is connected by USB cable to a computer equipped with CO2Meter.Inc GasLab 2.1 software, where raw measurements are recorded and can be displayed in real-time.

The CO2Meter GasLab® Pro Multi-Gas CM 1000 Data Logger

The CM 1000 Data Logger is a compact, integrated device that measures CO₂, O₂, CH₄, barometric pressure, temperature, dew point, and relative humidity. The three sensors, the pump, and the data-processing electronics are housed within a single unit (Fig. 3).

The device uses a small, battery-powered micro-pump to draw either atmospheric air or soil gas through its sensor chamber. Carbon dioxide and CH₄ sensors use infrared light absorption at a specific wavelength to measure concentration, whereas O₂ measurement uses fluorescence quenching by oxygen using a light source, a light detector, and a light-sensitive luminescent material. Each CO₂, O₂ or CH₄ sensor measurement is converted into concentration by the CM 1000 Data Logger's internal software, and the results are stored on a micro-SD card for later analysis.

A 25 mm nylon hydrophilic filter with a 0.45 µm pore size between the CM 1000 Data Logger inlet port and the atmospheric air inlet protects the sensors from damage by particulates in the airstream. Luer-Lok™ fittings allow rapid system changes to be made when alternating between sampling atmospheric air or soil gas.

COMPARISON OF ANALYTICAL RESULTS FROM THE SGAS AND CM 1000 DATA LOGGER

The SGAS and the CM 1000 Data Logger were compared by sampling soil gas at eleven different urban locations in Victoria, British Columbia. A typical test involved creating a vertical pilot hole with a 12.7-mm diameter pointed steel rod up to 30 cm into the soil. The soil probe was then driven 5 to 10 cm deeper into the soil before being withdrawn 1 cm to open the retractable tip, allowing soil gas flow. Before connecting the SGAS or the CM 1000 Data Logger to the probe, a small hand pump was used to confirm free flow of soil gas.

For SGAS measurements, the sensors were calibrated with the GasLab® 2.1 software using atmospheric CO₂ (~400 ppm) and O₂ (~209,050 ppm). The O₂ sensor manifold connects with a Luer-Lok™ to a 0.45 µm filter and a PVC tube through which atmospheric gas is sampled. The inlet is placed 100 cm away from the SGAS unit to avoid CO₂ contamination during calibration. Atmospheric CO₂ and O₂ concentrations are measured at 10 s intervals for two mins, during which the calibration occurs. The atmospheric inlet is then disconnected, and the O₂ sensor manifold inlet is connected to the soil probe. Soil gas CO₂ and O₂ concentrations are then pumped through the calibrated sensors and measured at 10 s intervals for another two mins. Typically, CO₂ increases from atmospheric levels and then plateaus, whereas O₂ levels concordantly decrease to a valley over the same interval (Fig. 4). The system is then switched back to measure atmospheric air for another two-minute interval following the soil gas measurements.

The CM 1000 Data Logger is calibrated by internal software to 400 ppm CO₂ and 20.95% O₂. Sampling atmospheric air or soil gas with the CM 1000 Data Logger is similar to the SGAS procedure. The CM 1000 Data Logger inlet port is connected through a 0.45 µm pore-size filter to a 100 cm long PVC tube for atmospheric air sampling. Variables are measured in atmospheric air every five seconds for one minute, and results are stored on the CM 1000 Data Logger's micro-SD card for later processing. The CM 1000 Data Logger inlet port is then connected to the soil probe and soil gas is sampled for one to two minutes. After which, the steel tube is disconnected, and atmospheric air is resampled for approximately one minute. Results are displayed in real-time on the CM 1000 Data Logger's display screen (Fig. 3).

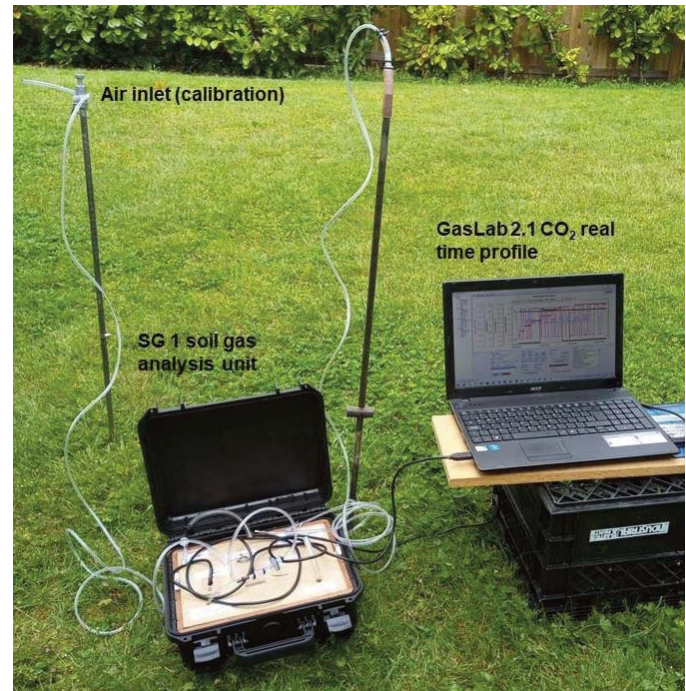


Fig. 2. Purpose-built 'SGAS' soil gas measurement system and laptop computer.



Fig. 3. Display and port hoses on the CO2Meter GasLab® Pro Multi Gas Sampling CM 1000 Data Logger.

CO₂ and O₂ in soil gas over faults, fractures and associated with mineralization *continued from p. 6*

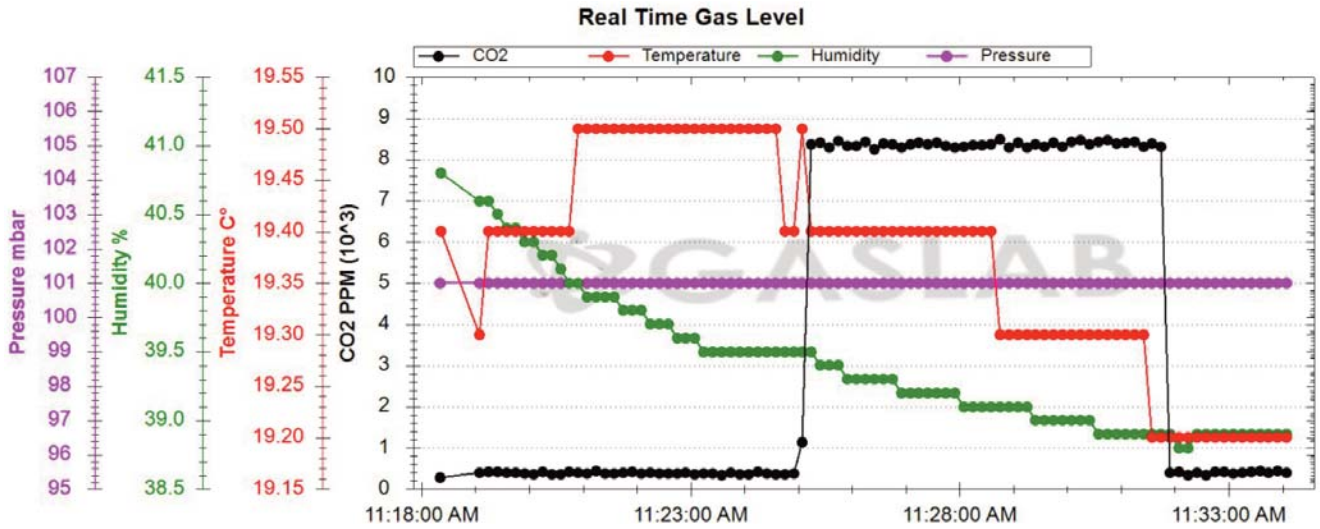


Fig. 4. Measurements of CO₂ in soil gas sampled at 40 cm depth, along with air pressure, humidity, and temperature obtained using the SGAS system at an urban test site in October, 2024.

The mean, range and percent relative standard deviation (%RSD) for CO₂ and O₂ concentrations recorded by the SGAS and the CM 1000 Data Logger at the same sites are presented in Table 1. These results reveal a 2% difference between the mean CO₂ measured by the two systems, but a 43% difference between the mean O₂. This large difference for O₂ may be a function of sensor measurement intervals, as the SGAS sensor can measure O₂ to 10 ppm whereas the CM 1000 Data Logger can only measure to 100 ppm O₂. Combined sampling and sensor precision can be expressed as an average coefficient of variation (%CV_{AVG}) (Abzalov 2008; Smee et al. 2024), where a value of <15% represents good precision, 15–30% represents acceptable precision, and >30% represents poor precision. The %CV_{AVG} calculated from the mean atmospheric air corrected CO₂ and O₂ values in the soil gas sampled with the SGAS and the CM 1000 Data Logger at eleven urban sites is 9.4% for CO₂ and 38.4% for O₂. The large %CV_{AVG} for O₂ indicates poor precision in O₂ measurements between devices, potentially as a function of the different detection limits.

Table 1. Comparison of soil gas analyzed for CO₂ and O₂ by the SGAS system and the CM 1000 Data Logger at urban sites.

System and measurement	Variable	Mean	Min	Max
SGAS	CO ₂ (ppm)	2515	630	7598
SGAS	CO ₂ %RSD	7.7	0.7	26.0
CM 1000 Data Logger	CO ₂ (ppm)	230	80	7600
CM 1000 Data Logger	CO ₂ %RSD	18.1	9.0	28.0
SGAS	O ₂ (ppm)	2610	900	5725
SGAS	O ₂ %RSD	0.6	0.2	1.5
CM 1000 Data Logger	O ₂ (ppm)	4100	100	7300
CM 1000 Data Logger	O ₂ %RSD	1.3	0.1	9.0

continued on page 8

CO₂ and O₂ in soil gas over faults, fractures and associated with mineralization *continued from p. 7*

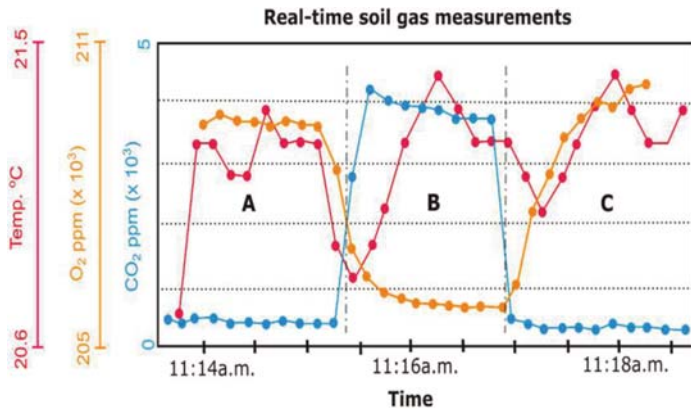


Fig. 5. A simplified example of GasLab 2.1® software display from the temporal analysis of soil gas and atmosphere for CO₂ (blue line), O₂ (orange line), and temperature (red line). The vertical grey lines roughly indicate the transition between atmosphere and soil gas measurements

SOIL GAS DATA PROCESSING

The aim of the data processing is to maximize the contrast between the rise in CO₂ and the reduction of O₂ amongst survey sites to accentuate anomalies. A measurement from a typical site is shown in Figure 5, where the first and last intervals are atmospheric measurements (sections A and C), and the middle interval (section B) is measured in soil gas. In this example, a total of 32 measurements were made over a period of about five minutes.

Soil gas survey results are typically displayed as the net soil gas CO₂ (ΔCO_2) and O₂ (ΔO_2) values, representing the difference between sensor-calibrated atmospheric gas and measured soil gas concentrations (Equations 1 and 2). The atmospheric A and C values in Equations 1 and 2 are mean values for the A and C datasets in Figure 5. The net ΔCO_2 & O₂ concentration in soil gas (Equation 3) provides a single variable for the combined variation in CO₂ and O₂ concentrations of the atmosphere and soil gases. The variation of CO₂ and O₂ in the gas emanating from faults may reveal additional information about associated mineralization, therefore ΔCO_2 and ΔO_2 are also evaluated individually.

$$\Delta\text{CO}_2 = \text{soil gas CO}_2 - \left[\frac{\text{Atmosphere[A] mean CO}_2 + \text{Atmosphere[C] mean CO}_2}{2} \right] \dots\{1\}$$

$$\Delta\text{O}_2 = \text{soil gas O}_2 - \left[\frac{\text{Atmosphere[A] mean O}_2 + \text{Atmosphere[C] mean O}_2}{2} \right] \dots\{2\}$$

$$\text{soil gas } \Delta\text{CO}_2 \& \text{O}_2 = \Delta\text{CO}_2 + \Delta\text{O}_2 \dots\{3\}$$

The Mouse Mountain soil gas and soil geochemistry survey

At Mouse Mountain (Fig. 1), soil gas and soil from the interface beneath the Ah (humus) soil horizon and above the B mineral horizon were collected at 33 sites at 10-m intervals along three transects. Disseminated chalcopyrite, pyrite, bornite, magnetite and malachite comprise the mineralized zone associated with a Jurassic calc-alkaline porphyry and a monzonite body. The monzonite intruded into Upper Triassic to Lower Jurassic Nicola Group potassic-altered sedimentary and volcanic rocks (Jonnes and Logan 2007). These rocks are fractured and faulted

continued on page 9

CO₂ and O₂ in soil gas over faults, fractures and associated with mineralization *continued from p. 8*

(Schimann 2014), but the exact location of a previously identified northeast-southwest- trending fault projected south of the Valentine zone is uncertain due to the overlying till veneer (<2 m) masking the bedrock. The survey lines are oriented perpendicular to the projected fault (Schimann 2014) in an area south of the Valentine Cu-Au porphyry-style sulphide mineralized zone (Fig. 6).

The samples collected at the Ah (humus) - B soil horizon interface were analyzed for a range of trace elements, including sulphur by inductively coupled plasma mass/emission spectrometry (ICPMS/ES) following a water leach (Lett et al. 2022). Soil pH was determined on a 1:1 v:v distilled water:soil slurry with a EutechOakion pHTestr^R metre. Analytical results for pH and sulphur reveal a spatial correlation with anomalous soil gas $\Delta\text{CO}_2\&\text{O}_2$ and sulphur (Lett et al. 2020). A higher inverse difference hydrogen (IDH) factor (Smee 1998, 2003, 2009), calculated from soil pH measurements, flanked by soil gas $\Delta\text{CO}_2\&\text{O}_2$ anomalies, suggests that greater CO₂ flow from a fault could be affecting soil chemistry (Fig. 7). Higher water-soluble sulphur levels, up to 10.5 ppm in soil, correspond with $\Delta\text{CO}_2\&\text{O}_2$ peaks along the westernmost N-S-oriented survey line (Fig. 7), which could be explained by sulphur gases such as SO₂ and carbonyl sulphide emanating from oxidizing sulphides associated with the fault (e.g. Hale 2010).

The Mount Milligan soil gas survey

At Mount Milligan, soil gas measurements were collected from 163 sites at 10 m intervals along north-south and southwest-northeast-oriented transects using the SGAS system (Fig. 8). The Mount Milligan survey area is underlain by Upper Triassic andesitic volcanic rocks of the Witch Lake succession (Logan et al. 2010). Centerra Gold Inc. subsequently trenched and completed geological mapping parallel to one of the soil gas survey transects. The mapping revealed monzonite dykes intruded into andesite flows and tuffs that were intersected by several fracture zones and veins (Fig. 8; Fitzgerald et al. 2020). Disseminated pyrite is common in these rocks and chalcopyrite appears in some fracture zones. Regionally, two faults are projected to cross the survey area, although their exact surface traces are uncertain due to overlying glacial sediments.

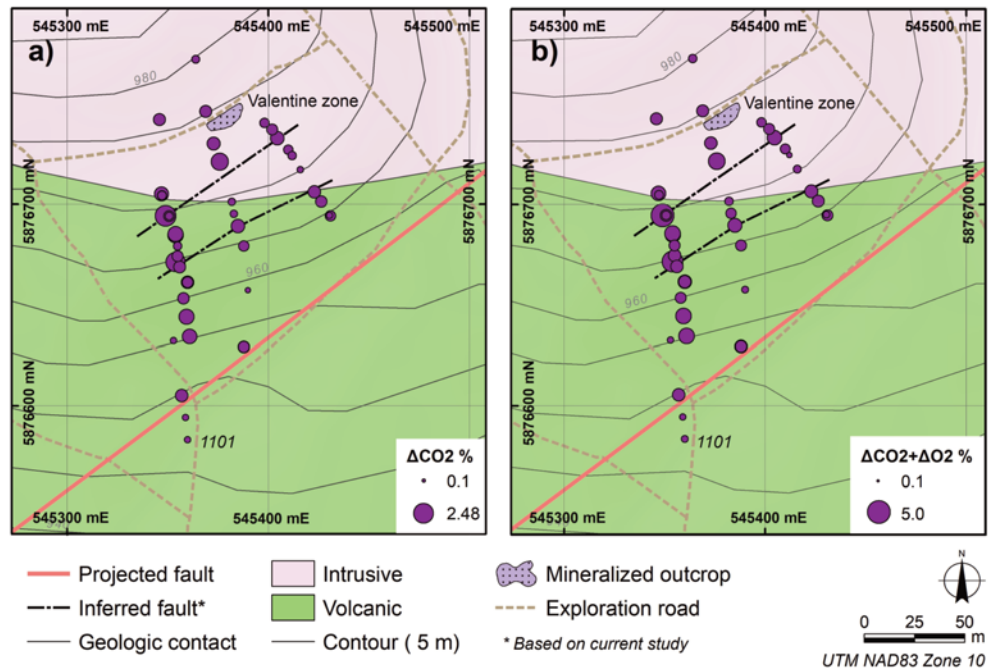


Fig. 6. Mouse Mountain geology (simplified from Schimann 2014), soil gas survey sites, (a) ΔCO_2 and (b) $\Delta\text{CO}_2\&\text{O}_2$ values measured in soil gas. Data displayed using proportional symbols.

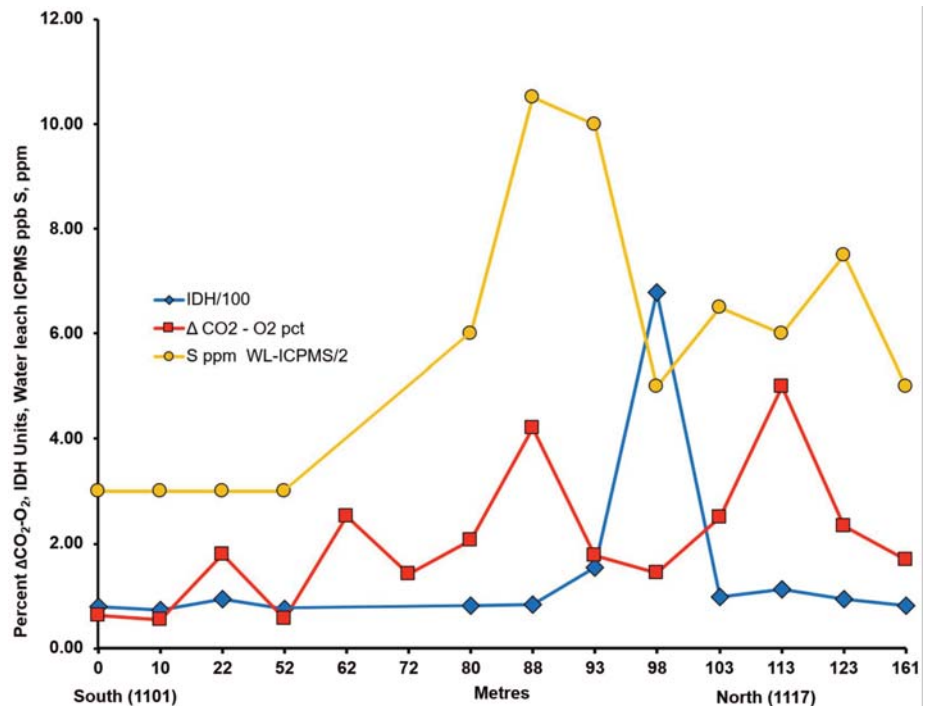
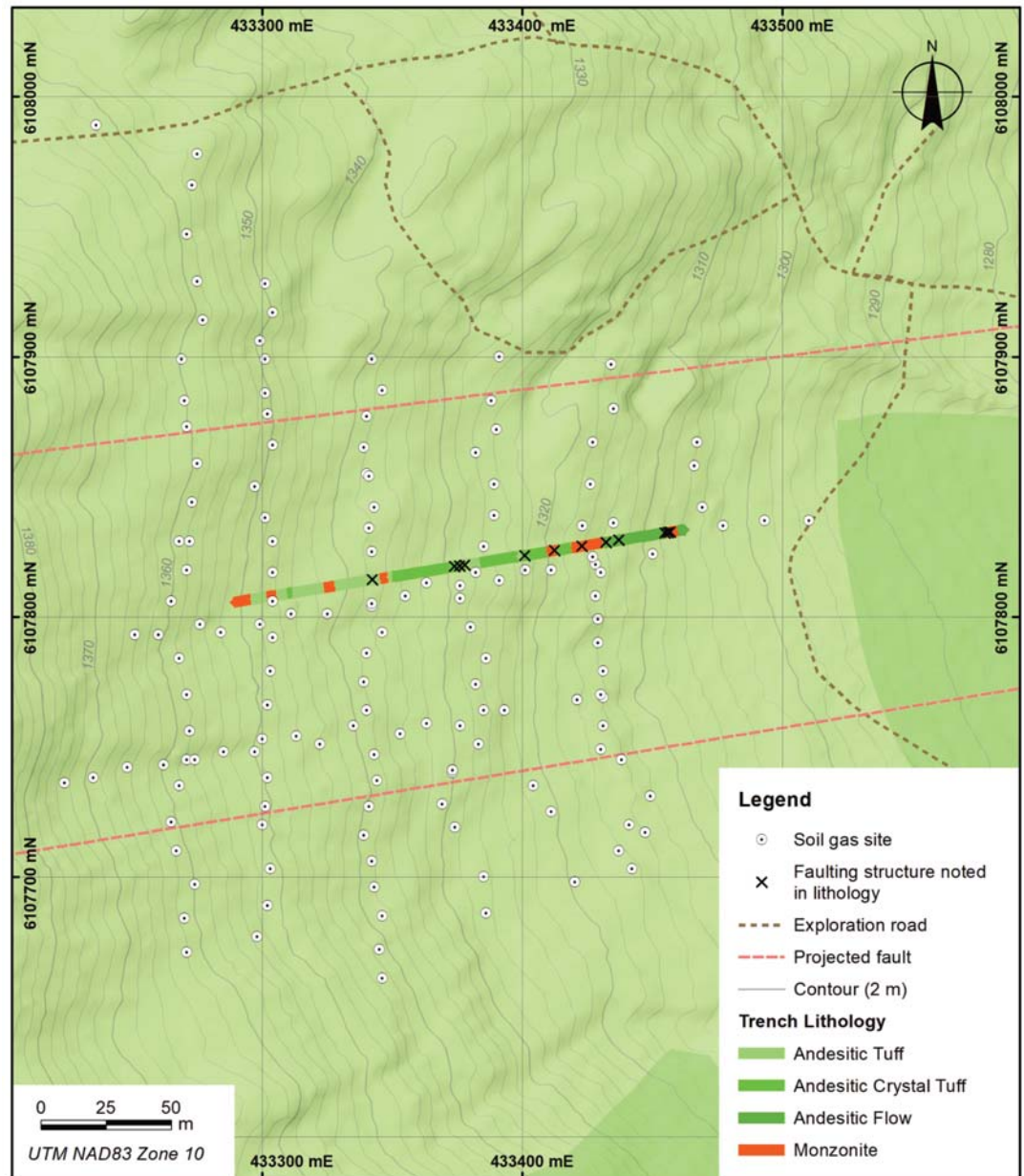


Fig. 7. Soil pH, expressed as inverse difference hydrogen (IDH), $\Delta\text{CO}_2\&\text{O}_2$ % and sulphur concentrations along the westernmost transect. Sulphur values have been divided by two to fit on the same axis.

CO₂ and O₂ in soil gas over faults, fractures and associated with mineralization *continued from p. 9*

Fig. 8. Soil gas measurement and projected fault locations from the 2020 and 2021 surveys on the Mount Milligan mine property and trench lithologies and fracture locations (mapping provided by Centerra Gold Inc.).



The Mount Milligan soil gas survey

At Mount Milligan, soil gas measurements were collected from 163 sites at 10 m intervals along north-south and southwest-northeast oriented transects using the SGAS system (Fig. 8). The Mount Milligan survey area is underlain by Upper Triassic andesitic volcanic rocks of the Witch Lake succession (Logan et al. 2010). Centerra Gold Inc. subsequently trenched and completed geological mapping parallel to one of the soil gas survey transects. The mapping revealed monzonite dykes intruded into andesite flows and tuffs that were intersected by several fracture zones and veins (Fig. 8; Fitzgerald et al. 2020). Disseminated pyrite is common in these rocks, and chalcopyrite appears in some fracture zones. Regionally, two faults are projected to cross the survey area, although their exact surface traces are uncertain due to overlying glacial sediments.

The sediment cover is a subglacial till veneer (<2 m thick) that thickens downslope to the east. The till is a compact diamicton composed of sandy-silt with angular to sub-rounded pebbles, cobbles, and boulders. On the eastern side of the survey area, the till was locally reworked by glacial meltwater that deposited a discontinuous, thin (20–50 cm), sandy mantle at surface. Brunisolic soil, which is the dominant soil in the local area, commonly has up to 15 cm of organic matter in its upper horizons, and the area supports an immature pine and fir tree forest. There are isolated bedrock outcrops in the western part of the survey grid, and more bedrock outcrops at surface about 150 m to the west of the grid.

Duplicate soil gas measurements were collected at eight of the sites. The %CV_{AVG} calculated from the atmospheric corrected duplicate soil gas CO₂ and O₂ values is 30.3% for ΔCO₂, 29.2% for ΔO₂ and 26.6% for ΔCO₂&O₂, which is bordering on poor precision. This low precision is attributed to local boulder-covered surfaces that precluded a tight seal around the soil probe in some locations.

CO₂ and O₂ in soil gas over faults, fractures and associated with mineralization continued from p. 10

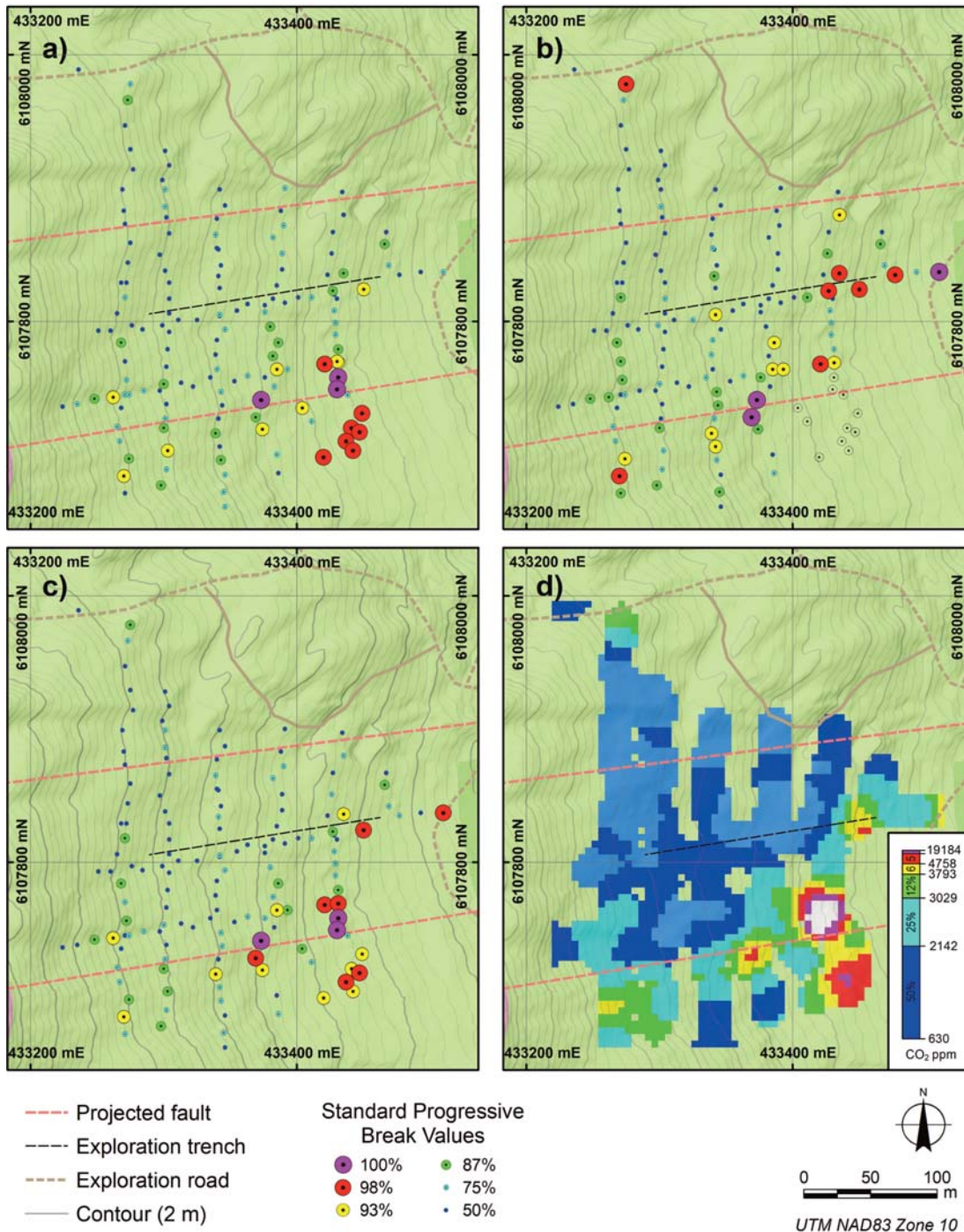


Fig. 9. Soil gas concentrations at the Mount Milligan Mine property. **a)** ΔCO_2 , **b)** ΔO_2 , **c)** $\Delta\text{CO}_2\&\text{O}_2$, and **d)** ΔCO_2 ppm gridded to 10 m pixels based on the maximum of a three-cell search radius smoothed across a two-cell radius. Proportional dot plots are displayed based on progressive percentile breaks. Gridded data symbolized using unequal bin percentile breaks of 30, 60, 80, 90, 95, 98, 99, 100.

Up to 1.9% ΔCO_2 and 2.16% $\Delta\text{CO}_2\&\text{O}_2$ were measured in the soil gas. The highest values are in the southern part of the survey area and are accompanied by lower ΔO_2 levels (Fig. 9). High $\Delta\text{CO}_2\&\text{O}_2$ values mark a target (Fig. 9c) with the centre of the roundel close to the trace of the projected southern fault. The contoured $\Delta\text{CO}_2\&\text{O}_2$ values reveal a trend aligned southwest-northeast that could be associated with this fault, which has a surface projection near the target. Since the fault location is projected to a flat surface from measurements in drill core, it is possible that the soil gas measurements represent a more accurate indication of the fault trace. Low ΔCO_2 and $\Delta\text{CO}_2\&\text{O}_2$ levels in the soil gas sampled in the area over the projected trace of the northern fault could be explained by the actual fault location beyond the survey limit, or that gas flow is inhibited by clay filling the structure.

The CO₂ and O₂ measured in soil gas at sites within a 20-m-wide buffer of the trench were compared to the trench logging results (Fig. 9 and 10). Several intervals of fracturing and veining are reported, including a zone of intense fractures towards the eastern end of the trench (~150–175 m on Fig. 9 and 10). This zone corresponds to sample sites with soil gas ΔCO_2 values over 4000 ppm and $\Delta\text{CO}_2\&\text{O}_2$ values over 8000 ppm, which are both around the 90th percentile of the dataset. Fracturing and/or veining identified at 67 m, 101 m, and ~125–150 m along the trench is also spatially correlative with ΔCO_2 and $\Delta\text{CO}_2\&\text{O}_2$ peaks. These results indicate that there is a correlation between fractures, veining, ΔCO_2

continued on page 12

CO₂ and O₂ in soil gas over faults, fractures and associated with mineralization *continued from p. 11*

and $\Delta\text{CO}_2\&\text{O}_2$. Depletion of O₂ with concomitant CO₂ increases (Fig. 11) suggests sulphide mineralization in some fractured areas, particularly at 175 m.

The Anita soil gas survey

In April and June 2024, soil gas was measured at 40 sites using the CM 1000 Data Logger (Fig. 12) on the Anita property, southern Vancouver Island, British Columbia (Fig. 1). The survey was completed along two transects, crossing northwest-southeast-trending faults and a buried Cu-Pb-Zn-Au-Ag massive sulphide horizon. Soil gas was measured at 15 m intervals from 20 sites along the western transect on April 20th, 2024, and 20 sites along the eastern transect on June 30th, 2024 (Fig. 12).

The property is underlain by felsic and mafic metavolcanic rocks of the McLaughlin Ridge Formation (MRF), which is the uppermost unit of the Paleozoic Sicker Group. The MRF is equivalent to the Myra Formation, which is the host for the sulphide mineralization at the Myra Falls Cu-Pb-Zn mine, central Vancouver Island. Property geology includes tuffs, coarse fragmental volcanic rocks, massive flows, intrusive rocks and minor sedimentary rocks intruded by numerous gabbroic dykes. The volcanic rocks have sericite-, pyrite- and chlorite-alteration, and have undergone several periods of deformation to form the core of a west-northwest-trending, west-plunging anticlinal structure. Numerous late brittle faults, and a southwest-verging reverse fault, thought to be a splay of the Fulford Thrust fracture, crosscut the anticline. A sequence of pyritic (2–50%), moderately to strongly sericitized, Ba-enriched, Na₂O-depleted felsic lapilli tuffs, referred to informally as the 'Anita Active Tuff' (AAT), host up to 25% of sulphide minerals comprising pyrite ± pyrrhotite + sphalerite + chalcopyrite ± galena (Nelles 2024).

The survey area was recently logged, and immature western hemlock and shrubs dominate the surface. Brunisolic soils have developed on a thin subglacial till veneer (<2 m thick), and there are patches of organic-rich soil along a stream channel across the northern part of the survey area.

The CO₂ and O₂ results were processed to calculate ΔCO_2 , ΔO_2 and $\Delta\text{CO}_2\&\text{O}_2$ values. The %CV_{AVG} for the CO₂ and O₂ duplicate samples was 16.9% for soil gas CO₂; 12.74% for atmospheric CO₂; 0.66% for soil gas O₂; and 0.21% for atmospheric O₂, indicating good to acceptable precision.

Strong ΔCO_2 , and $\Delta\text{CO}_2\&\text{O}_2$ anomalies associated with weaker ΔO_2 anomalies occur towards the south end of both transects, with values up to 1.8% ΔCO_2 and 4.9% $\Delta\text{CO}_2\&\text{O}_2$ (Fig. 13). The ΔCO_2 and $\Delta\text{CO}_2\&\text{O}_2$ peaks correspond re-

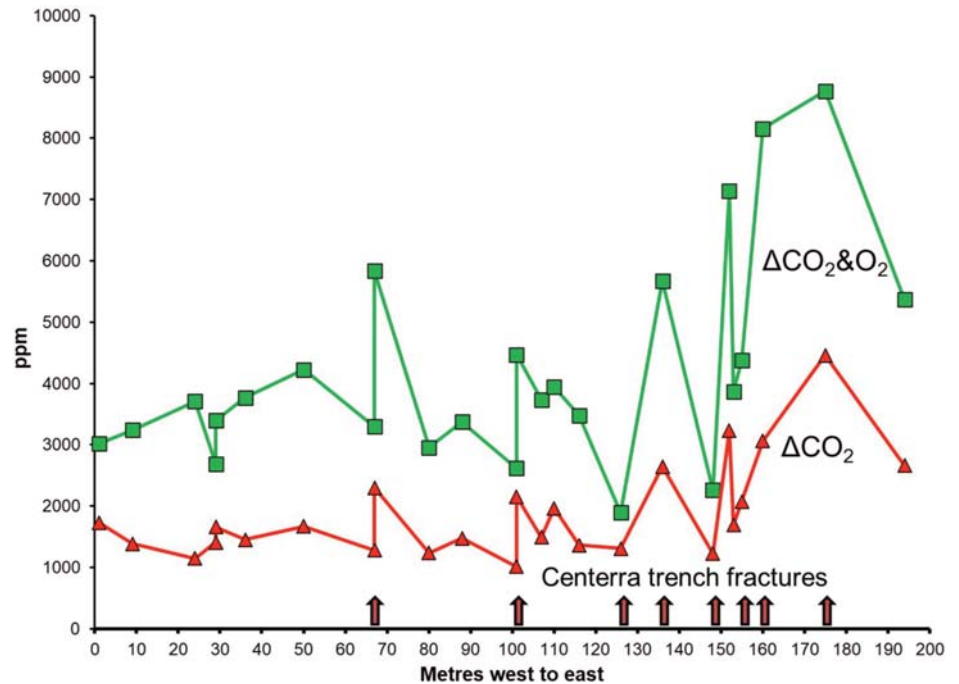


Fig. 10. The variation of ΔCO_2 and $\Delta\text{CO}_2\&\text{O}_2$ in the soil gas at sites within a 20 m wide buffer along the mapped bedrock trench. Trenching was completed after the soil gas measurements.

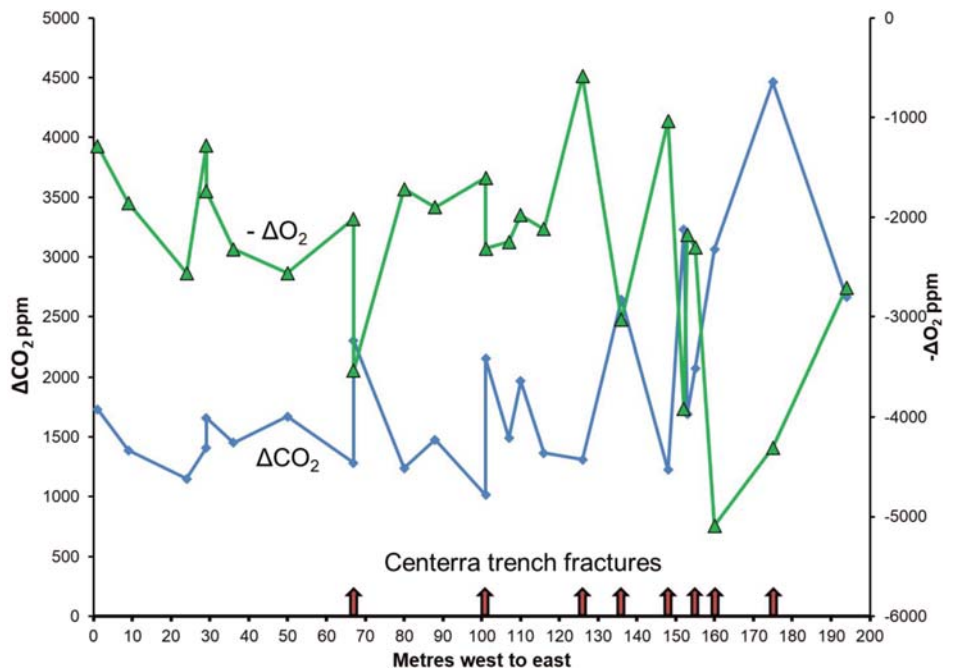


Fig. 11. The variation of ΔCO_2 and the ΔO_2 (expressed as a negative) at sites within a 20 m wide buffer along the mapped bedrock trench demonstrates the increase in CO₂ and concomitant reduction in O₂ associated with fractures. The highest values around 175 m may indicate sulphide mineralization.

CO₂ and O₂ in soil gas over faults, fractures and associated with mineralization *continued from p. 12*

sonably well to the interpreted projection of a northwest- to southeast-trending fault crossing the area. The southern anomaly cluster on the western transect is displaced 35 m north of the interpreted fault trace. The northern displacement of this peak may indicate that the actual fault location is farther north or that gas flows laterally from the fault through the glacial sediment to reach the surface. Similar anomalies on the southern part of the eastern transect suggest the fault may continue east.

Smaller ΔCO_2 , and $\Delta\text{CO}_2\&\text{O}_2$ peaks towards the centre of both transects correspond to the interpreted surface projection of a sulphide mineralized horizon (Fig. 13). At the transects' northern ends, high ΔCO_2 values may result from gas generated from organic soil decomposition along a poorly drained stream draw. No CH₄ was detected in the soil gas.

DISCUSSION

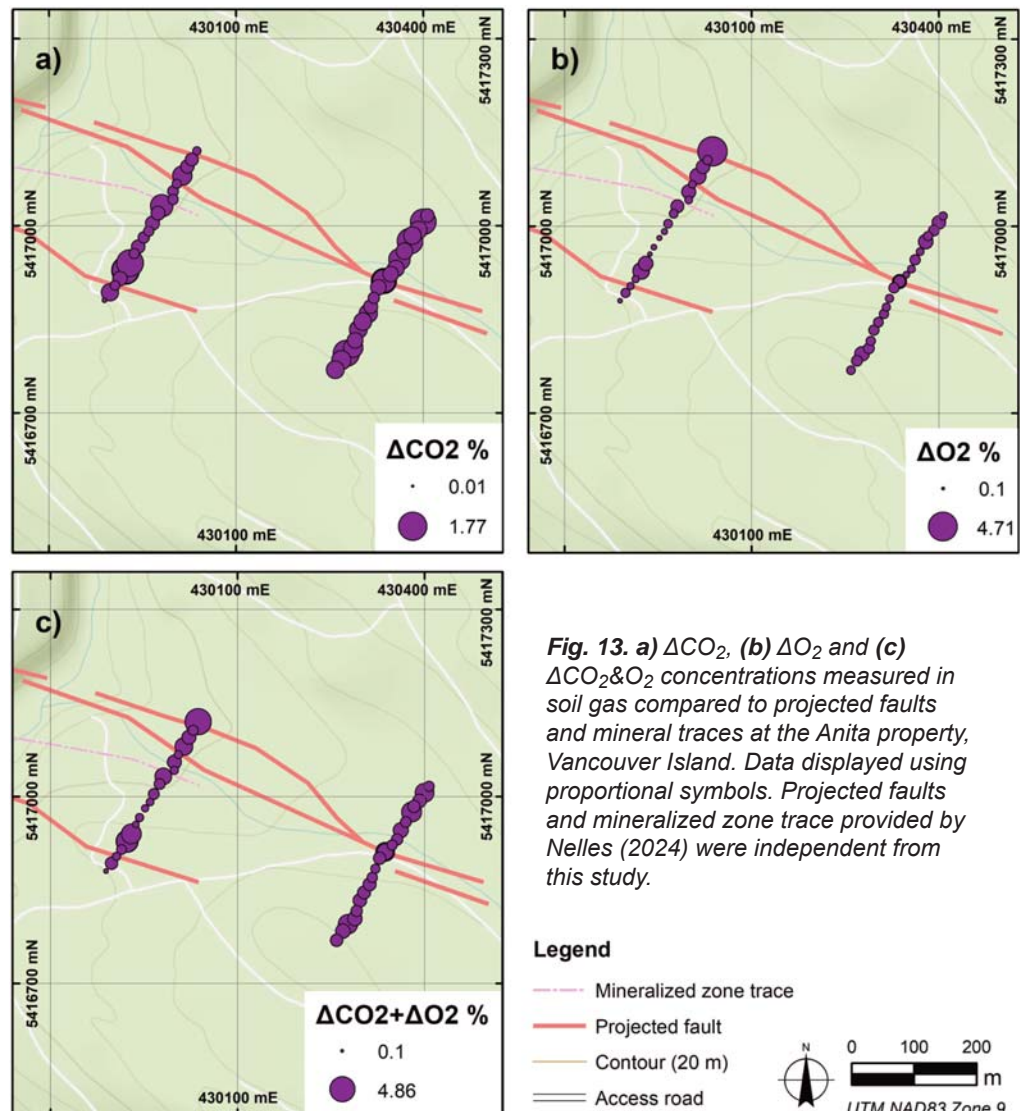
There is a strong spatial correlation of positive ΔCO_2 and negative ΔO_2 soil gas anomaly peaks with the fracturing mapped in a trench at Mount Milligan and the projected faults at Anita. The association between the projected fault trace and soil gas chemistry is more subtle at Mouse Mountain; however, stronger anomalies suggest the occurrence of additional faults or fractures to the north of the projected fault.

There are several external factors that could cause variation in CO₂ and O₂ concentration, such as changes in soil moisture, biological activity, sample depth, landscape and time of day (Hodges et al. 2019). For example, at Anita in April 2024, the atmospheric CO₂ increased from 474 ppm late morning to 783 ppm in early afternoon and then declined to 535 ppm later in the afternoon. Though the diurnal CO₂ variation at Anita would have little effect on anomaly contrast, given the percent CO₂ measured in soil gas, the fluctuation illustrates a need to consider daily background variation when interpreting the results of soil gas surveys. Ideally, a base station monitoring daily CO₂-O₂ fluctuation could be used, but would increase the costs for a survey in terms of equipment and field personnel. Additionally, interference due to an inconsistent seal between the soil probe and sediment could affect measured values, as suggested by the poor precision calculated at Mount Milligan.

Although the results of the Mount Milligan and Anita soil gas



Fig. 12. Collecting soil gas for CO₂, O₂ and CH₄ analysis using the CO₂Meter GasLab® Pro Multi-Gas CM 1000 Data Logger on the Anita property.



CO₂ and O₂ in soil gas over faults, fractures and associated with mineralization *continued from p. 13*

surveys suggest the detection of faults and fractures, it is unclear if the results distinguish between structures that host sulphide mineralization from those that are barren. Detecting Hg vapour (e.g. Rukhlov 2022) or gaseous sulphur species (e.g. Hale 2010; Plet et al. 2021) could improve the ability of soil gas surveys to discriminate between sulphide mineralized and non-mineralized structures.

Experiments by Plet et al. (2021) and Hinkle et al. (1990) demonstrated that CO₂, SO₂, carbonyl sulphide (COS), and carbon disulphide (CS₂) are generated from aerobic and anaerobic weathering of different sulphide minerals, including pyrite and chalcopyrite. Research by Cox et al. (2013) into the biodegradation of CS₂ in soil revealed COS formed first (Equation 4) followed by H₂S (Equation 5) and ultimately H₂SO₄ (Equation 6).



Water-soluble sulphur levels in soils of up to 10.5 ppm associated with a ΔCO₂&O₂ peak at Mouse Mountain could reflect SO₄ in the soil from oxidation of fault-hosted sulphide minerals to CS₂ and eventually H₂SO₄. An analysis of a soil water leach for SO₄ could provide a basis to differentiate soil gas CO₂ and O₂ anomalies associated with sulphide mineralization from barren faults. Soil pH at Mouse Mountain appears to have a relationship with higher ΔCO₂&O₂ as suggested by Beaubien (2008); however, the number of pH determinations is insufficient to confirm the relationship.

CONCLUSIONS

Two systems, the SGAS and the CM 1000 Data Logger, were used to measure CO₂ and O₂ in soil gas. A comparison of soil gas analyzed for CO₂ and O₂ using the SGAS and the CM 1000 Data Logger systems show similar results, although O₂ is less sensitive when measured with the CM 1000 Data Logger. The lower sensitivity may be due to a 10 ppm SGAS O₂ sensor detection limit compared to the 100 ppm O₂ detection limit of the CM 1000 Data Logger.

Soil gas surveys over the Mount Milligan Cu-Au deposit and the Anita Cu-Pb-Zn-Au-Ag VMS mineral property reveal some spatial relationship between mapped faults and elevated ΔCO₂ and ΔCO₂&O₂ and negative ΔO₂. At Mouse Mountain, additional potential fault locations have been interpreted from the results of the soil gas survey. Additionally, higher sulphur in soil water extracts corresponding to the elevated ΔCO₂ and lower ΔO₂ in the soil gas may indicate sulphur gases emanating from weathering sulphides migrating along faults to the surface. It is concluded that both the commercial and purpose-built real-time soil gas measurement systems provide a promising methodology for detect the surface trace of buried structures. With additional survey refinements and the inclusion of additional variables (e.g. soil pH, or geochemistry; other soil gases such as SO₂, Hg), it may also be possible to detect which structures are associated with sulphide mineralization.

continued on page 15

CO₂ and O₂ in soil gas over faults, fractures and associated with mineralization *continued from p. 14***ACKNOWLEDGEMENTS**

Funding for the development of SGAS system and for the Mouse Mountain survey by Geoscience BC is very much appreciated by the authors. W. Jackaman, Principle, Noble Exploration Services Ltd. kindly advised and helped the senior author during an initial test of the SGAS system over the Leach River Fault, BC. Permission from K. Schimann, CanAlaska Uranium, to access the Mouse Mountain property is appreciated. J. Houck, CO2Meter Inc., is thanked for his invaluable advice on the use of the SGAS system sensors and the CM 1000 Data Logger. Centerra Gold Inc. staff at the Mount Milligan mine are especially thanked for their support during the surveys. Support and advice from D. Nelles and T. Setterfield for the Anita property soil gas sampling in 2024 is very much appreciated. Special thanks to Dr. Ryan Noble (CSIRO), Beth McClenaghan and Lyndsay Moore (Geological Survey of Canada) for their constructive suggestions during a review of the paper.

REFERENCES

- Abzalov, M. 2008. Quality control of assay data: a review of procedures for measuring and monitoring precision and accuracy. *Exploration and Mining Geology*, **17**, 131–144. <https://doi.org/10.2113/gsemg.17.3-4.131>
- Annunziatellis, A., Beaubien, S.E., Bigi, S., Ciotoli, G. M., Coltella, M. and Lombardi, S. 2008. Gas migration along fault systems and through the vadose zone in the Latera caldera (central Italy). Implications for CO₂ geological storage. *International Journal of Greenhouse Gas Control*, **2**, 353–372. <https://doi.org/10.1016/j.ijggc.2008.02.003>
- Beaubien, S.E., Ciotoli, G., Coombs, P., Dictor, M.C., Kruger, M., Lombardi, S., Pearce, J.M. and West, J.M. 2008. The impact of a naturally occurring CO₂ gas vent on the shallow ecosystem and soil chemistry of a Mediterranean pasture (Latera, Italy). *International Journal of Greenhouse Gas Control*, **2**, 373–387. <https://doi.org/10.1016/j.ijggc.2008.03.005>
- Cox, S.F., McKinley, J.D., Ferguson, A.S., O'Sullivan, G. and Kalin, R.M. 2013. Degradation of carbon disulphide (CS₂) in soils and groundwater from a CS₂ - contaminated site. *Environmental Earth Sciences*, **68**, 1935–1944. <https://doi.org/10.1007/s12665-012-1881-y>
- Fitzgerald, J., Jago, P.C., Jankovic, B., Simonian, B., Taylor, C.A. and Borntraeger, B. 2020. Technical report on the Mount Milligan mine, North-Central BC. Centerra Gold Inc. NI 43-101 Technical Report 268.
- Hale, M. 2010. Gas geochemistry and deeply buried mineral deposits: the contribution of the Applied Geochemistry Research Group, Imperial College of Science and Technology, London. *Geochemistry: Exploration, Environment, Analysis*, **10**, 261–267. <https://doi.org/10.1144/1467-7873/09-236>
- Highsmith, P. 2004. Overview of soil gas theory. *EXPLORE*, Newsletter of the Association of Exploration Geochemists, **122**, 1–15.
- Hinkle, M.E., Ryder, J.L., Sutley, S.J and Botinelly, T. 1990. Production of sulfur gases and carbon dioxide by synthetic weathering of crushed drill cores from the Santa Cruz porphyry copper deposit near Casa Grande, Pinal County, Arizona. *Journal of Geochemical Exploration*, **38**, 43–67. [https://doi.org/10.1016/0375-6742\(90\)90092-O](https://doi.org/10.1016/0375-6742(90)90092-O)
- Hodges, G., Kim, H., Brantley, S.L. and Kaye, J. 2019. Soil CO₂ and O₂ concentrations illuminate the relative importance of weathering and respiration to seasonal soil gas fluctuations. *Journal of the Soil Science Society of America*, **83**, 1167–1180. <https://doi.org/10.2136/sssaj2019.02.0049>
- Jonnes, S. and Logan, J.M. 2007. Bedrock geology and mineral potential of Mouse Mountain, central British Columbia. In: Geological Fieldwork 2006. British Columbia Ministry of Energy, Mines and Petroleum Resources, BC Geological Survey, Paper 2007-1, 55–66. <https://www2.gov.bc.ca/gov/content/industry/mineral-exploration-mining/british-columbia-geological-survey/publications/fieldwork>
- Kesler, S.E., Gerdenich, M.J., Steininger, R.C. and Smith, C. 1990. Dispersion of soil gas around micron gold deposits. *Journal of Geochemical Exploration*, **38**, 117–132. [https://doi.org/10.1016/0375-6742\(90\)90096-S](https://doi.org/10.1016/0375-6742(90)90096-S)
- Lett, R.E., Sacco, D.A., Elder, B. and Jackaman, W. 2020. Real-time analysis of soil gas for carbon dioxide and oxygen to identify bedrock mineralization and geological faults beneath glacial deposits in central British Columbia. Geoscience BC, Report 2020-07, 50. <https://www.geosciencebc.com/projects/2018-028/>
- Lett, R.E., Sacco, D.A., Elder, B. and Knox, C. 2022. Developments in the real-time detection of buried mineralization and geological structures using soil gas concentrations. Geoscience BC, Report 2022-12, 34. <https://www.geosciencebc.com/projects/2018-028/>

CO₂ and O₂ in soil gas over faults, fractures and associated with mineralization *continued from p. 15*

- Logan, J.M., Schiarizza, P.A., Struik, L.C., Barnett, C., Nelson, J.L., Kowalczyk, P., Ferri, F., Mihalyuk, M.G. et al. 2010. Bedrock geology of the QUEST map area, central British Columbia. British Columbia Geological Survey, Geoscience Map 2010-01; Geological Survey of Canada, Open File 6476.
- Lovell, J.S., Hale, M. and Webb, J.S. 1979. Soil air disequilibrium as a guide to concealed mineralization at Keel, Eire. *In: Prospecting in Areas of Glaciated Terrain*, 1979. The Institute of Mining and Metallurgy, London, 45–50.
- Lovell, J.S., Hale, M. and Webb, J.S. 1980. Vapour geochemistry in mineral exploration. *The Mining Magazine*, **143**, 229–239.
- McCarthy, J.H., Lambe, R.N. and Dietrich, J.A. 1986. A case study of soil gases as an exploration guide in glaciated terrain: Crandon massive sulfide deposit, Wisconsin. *Economic Geology*, **81**, 408–420. <https://doi.org/10.2113/gsecongeo.81.2.408>
- Nelles, D.M. 2024. Report on the 2024 Preliminary Soil Gas Survey on the Anita Property. British Columbia Ministry of Energy and Mines and Critical Minerals, Assessment Report 42562, 23. <https://apps.nrs.gov.bc.ca/pub/aris/Report/42562.pdf>
- Plet, C. and Nobel, R.R.P. 2023. Soil gases in mineral exploration: a review and the potential for future developments. *Geochemistry: Exploration, Environmental, Analysis*, **23**, 1–17. <https://doi.org/10.1144/geochem2023-008>
- Plet, C., Siegel, C., Woltering, M., Noble, R., Pages, A., Thorne, R., Spinks, S. and Anand, R. 2021. Sulfur and CO₂ gases emitted during weathering of sulfides: Role of microbial activity and implications to exploration through cover. *Ore Geology Reviews*, **134**, 1–11. <https://doi.org/10.1016/j.oregeorev.2021.104167>
- Rukhlov, A.S., Ootes, L., Hickin, A.S. and Mashyanov, N.R. 2021. Near-surface mercury vapour haloes in air above ore deposits and faults on Vancouver Island: Insights into buried materials in real-time? *In: Geological Fieldwork 2020*. British Columbia Ministry of Energy, Mines and Petroleum Resources, Paper 2021-01, 30–143.
- Schimann, K. 2014. Geology and geochemistry at the QM property, NTS: 93G 01, British Columbia. British Columbia Ministry of Energy, Mines and Petroleum Resources, Assessment Report 35262, 28.
- Smee, B.W. 1998. A new theory to explain the formation of soil geochemical response over deeply covered gold mineralization in arid environments. *Journal of Geochemical Exploration*, **61**, 149–172. [https://doi.org/10.1016/S0375-6742\(98\)00007-7](https://doi.org/10.1016/S0375-6742(98)00007-7)
- Smee, B.W. 2003. Theory behind the use of soil pH measurements as an inexpensive guide to buried mineralization, with examples. *EXPLORE*, Newsletter of the Association of Exploration Geochemists, **118**, 1–18.
- Smee, B.W. 2009. Soil micro-layer, airborne particles and pH: the Govett connection. *In: Lentz, D.R., Thorne, K.G. and Beal, K.L. (ed.) Proceedings of the 24th International Applied Geochemistry Symposium, June 1–4, 2009, Fredericton, New Brunswick*, 1, 91–95.
- Smee, B.W., Bloom, L., Arne, D. and Heberlein, D. 2024. Practical applications of quality assurance and quality control in mineral exploration, resources estimations and mining programs: a review of recommended international practices. *Geochemistry: Exploration, Environmental, Analysis*, **24**, 1–21. <https://doi.org/10.1144/geochem2023-046>
- Zhao, X., Deng, H., Wang, W. et al. 2017. Impact of naturally leaking carbon dioxide on soil properties and ecosystems in the Qinghai-Tibet plateau. *Nature Scientific Reports*, **7**, 3001. <https://doi.org/10.1038/s41598-017-02500-x> 